

Preparation of CNTs / Aluminum Foam Composites

Zhaoyang Lang¹, Mingying Chen¹, Junjiao Han¹, Zhe Liu¹, Xiaoqin Yan¹,
Yousong Gu¹, Zhen Ji¹ and Chengchang Jia¹

¹) School of Materials Science and Engineering, University of Science and Technology
Beijing, Beijing, 100083, China

Corresponding author's: lang_zy5992@163.com

Abstract. This article uses powder metallurgy to prepare aluminum foam and carbon nanotubes (CNTs) / foam aluminum composites. The effects of the surface treatment of carbon nanotubes, the amount of pore-forming agent, and the amount of carbon nanotubes on the microstructure of aluminum foam and its composites were studied by means of infrared spectroscopy, Raman spectroscopy, and scanning electron microscopy. The results show that the mixed acid treatment of CNTs can effectively disperse CNTs and introduce new functional groups on their surfaces. Using NH_4HCO_3 as a pore-forming agent and using powder metallurgy, a porosity of 41% to 79%, Cellular pure foam aluminum material and CNTs / foam aluminum matrix composite with 60% porosity.

1. Introduction

Aluminum foam has many advantages such as low density, high specific surface area and corrosion resistance. Therefore, it is widely used in automobile manufacturing, ship hull, aerospace materials, construction and chemical industry [1-3]. Due to its excellent mechanical properties, carbon nanotubes (CNTs) can be used as a lightweight reinforcing phase to improve the mechanical properties of aluminum foam.

The preparation methods of aluminum foam include liquid phase method, solid phase method and electrolytic deposition method [4]. However, it is not easy to obtain the microstructure of aluminum foam with uniform pore distribution and fewer defects. Due to the low mechanical properties of pure aluminum foam, it is necessary to add the reinforcing phase to make aluminum foam composite material, which makes the preparation process more complicated.

This article uses powder metallurgy to prepare aluminum foam and carbon nanotube / aluminum foam composites. The effects of surface treatment, pore-making agent and addition of carbon nanotubes on microstructure of aluminum foam and its composites were studied by infrared spectroscopy, Raman spectroscopy, and scanning electron microscopy and other characterization methods, providing experimental support for future studies on aluminum foam.

2. Experiment

2.1. Experimental Materials

Aluminum powder was purchased from Beijing Xingrongyuan Co., Ltd. The particle size was 600 mesh, the average diameter was about 23 μm , and the purity was > 99.7%, as shown in Figure 1. CNTs were purchased from Deco Island Gold Co., Ltd., with a length of 20-30 μm and a purity of 97%. The pore-forming agent is NH_4HCO_3 .



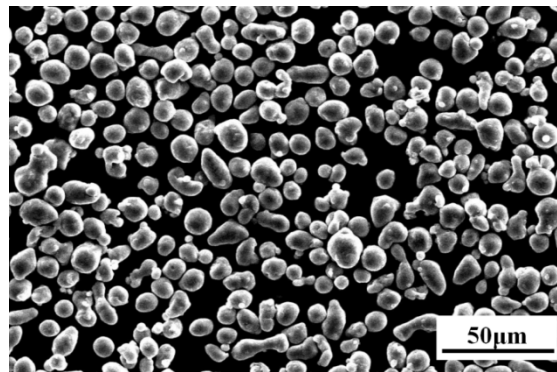


Figure 1. SEM photo of aluminum powder

2.2. Experimental Method

Pure aluminum foam was prepared by powder metallurgy. First weigh a certain mass of aluminum powder and pore-forming agent NH_4HCO_3 , where the mass fraction of NH_4HCO_3 is 30% ~ 70%, then mix the two evenly, put it into an alloy steel mold with a diameter of 30mm, and press-mold at 400MPa pressure. The pore-forming agent is dried and decomposed at low temperature, and the preform body is finally sintered in a tube furnace with argon gas to obtain a small-pore foam aluminum material with certain pores.

Carbon nanotubes / foam aluminum composites were prepared by powder metallurgy method. A certain quality aluminum powder and a CNTs surface treated with concentrated sulfuric acid and concentrated nitric acid and 0.25%~1.5% of mass fraction were first mixed. The mixture was mixed in the mixer and added to NH_4HCO_3 . Then the CNTs reinforced small pore aluminum foam material with porosity of 60% was prepared according to the above method.

2.3. Characterization Method

Raman spectroscopy and infrared spectroscopy were used to analyze the surface structure of the surface modified carbon nanotubes. The microstructure, CNTs distribution and pore size of foam aluminum composites were observed by JSM-6510A scanning electron microscope and NeXView three-dimensional white light interferometer.

3. Experimental Results and Analysis

3.1. Surface Analysis of Modified CNTs

Figure 2 is a SEM photograph of CNTs before and after acid treatment. It can be seen that the CNTs after acid treatment are no longer entangled with each other like the original CNTs, and the dispersion is effectively improved.

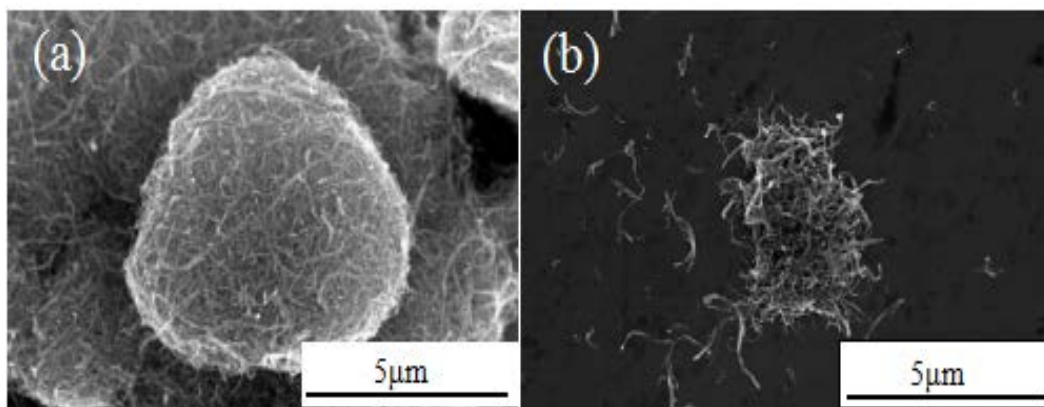


Figure 2. SEM photos of CNTs before (a) and after (b) mixed acid treatment

Figure 3 is the photo of alcohol suspension before and after CNTs surface treatment. It can be found that the original CNTs suspension has completely precipitated after standing for 1h, while the treated CNTs suspension has not been completely deposited after standing for 10h, which may be due to the introduction of some hydrophilic functional groups on the surface of CNTs after treatment, so that CNTs can be more completely dispersed.

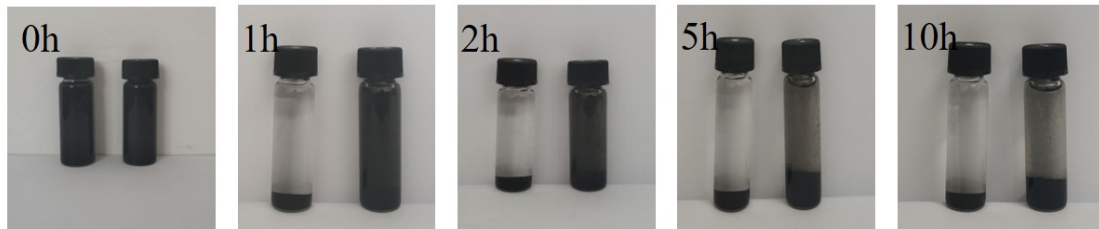


Figure 3. Photos of alcohol suspension before and after mixed acid treatment

Infrared spectrum test was carried out on CNTs before and after treatment. From the curve in Figure 4, it can be seen that the untreated CNTs have the stretching vibration peak of carbon oxygen double bond in the carboxyl group at 1622cm^{-1} , the absorption peak of hydroxyl group at 3427cm^{-1} , and the peak at 2921cm^{-1} is $-\text{CH}_2$ symmetric and antisymmetric vibration peak, indicating that there will be a small amount of hydroxyl and carboxyl containing functions on the surface of CNTs prepared by CVD Group [5]. Compared with the original CNTs, the intensity of the treated CNTs is large and broad, and a new carbon-oxygen double bond stretching vibration peak appears at 1067cm^{-1} [6], indicating that the treated CNTs are not only purified, but also new oxygen-containing functional groups were introduced on its surface, which made the distance between CNTs larger, and it was easier to achieve the dispersion effect [7-9].

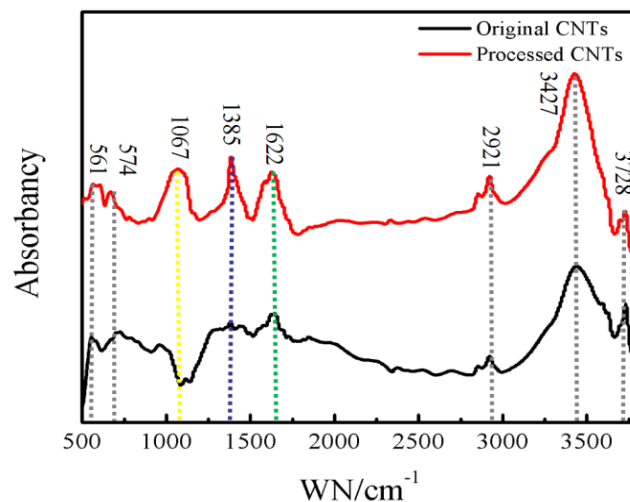


Figure 4. Infrared spectrum of CNTs before and after mixed acid treatment

Figure 5 shows the Raman spectrum of CNTs at 1000cm^{-1} to 3000cm^{-1} before and after mixed acid treatment. Three strong peaks appear in the figure. The peak at 2680cm^{-1} corresponds to the double wave number of the D peak, and is also called the G' peak. The Raman frequency shift of the G' peak is related to the excitation wavelength [10]. The peaks at 1346cm^{-1} and 1571cm^{-1} represent the D peak of the carbon atom lattice defect in the CNTs and the G peak of the graphitized structure. The ratio of the two peaks, i.e. I_D / I_G , represents the ratio of amorphous to crystalline carbon content in CNTs, which can be used to characterize the structural changes of CNTs [11]. The I_D / I_G of CNTs increased from 0.69 to 0.79 before and after mixed acid treatment, indicating that defects were

generated on the surface of CNTs, the reactivity was enhanced, it was easier to introduce oxygen-containing functional groups, and the dispersibility of CNTs was better.

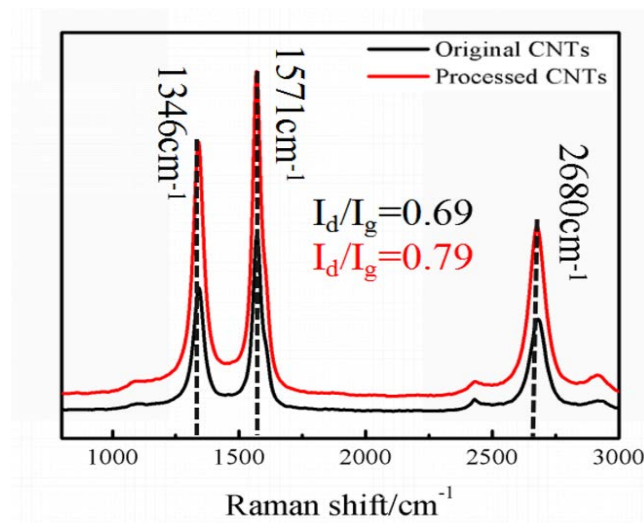


Figure 5. Raman diagrams of CNTs before and after mixed acid treatment

3.2. Effect of Pore Former Mass Fraction on Microstructure of Aluminum Foam

Figure 6 is a histogram of the porosity of aluminum foam prepared by adding different mass fractions of NH_4HCO_3 . It can be seen that as the mass fraction of NH_4HCO_3 increases, foamed aluminum materials with porosity from 41% to 79% can be obtained.

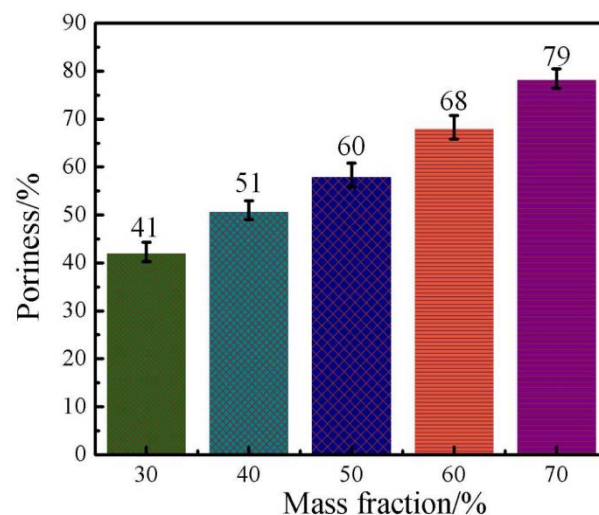


Figure 6. Porosity histogram of foamed aluminum with different mass fraction of NH_4HCO_3

Figure 7 shows the SEM photographs of the different porosity aluminum foams and their corresponding three dimensional photographs. It can be seen from Fig. 7a that the distribution of pores is even more uneven with the increase of the porosity of the foam aluminum, and even the structure of the pores is destroyed. In Fig. 7b, different interference colors represent different depths of the surface, and the size of the aperture can be calculated by the relative value of the corresponding color. It can be seen that the pore size does not change significantly with the increase of porosity, and the maximum pore size is about 400 μm .

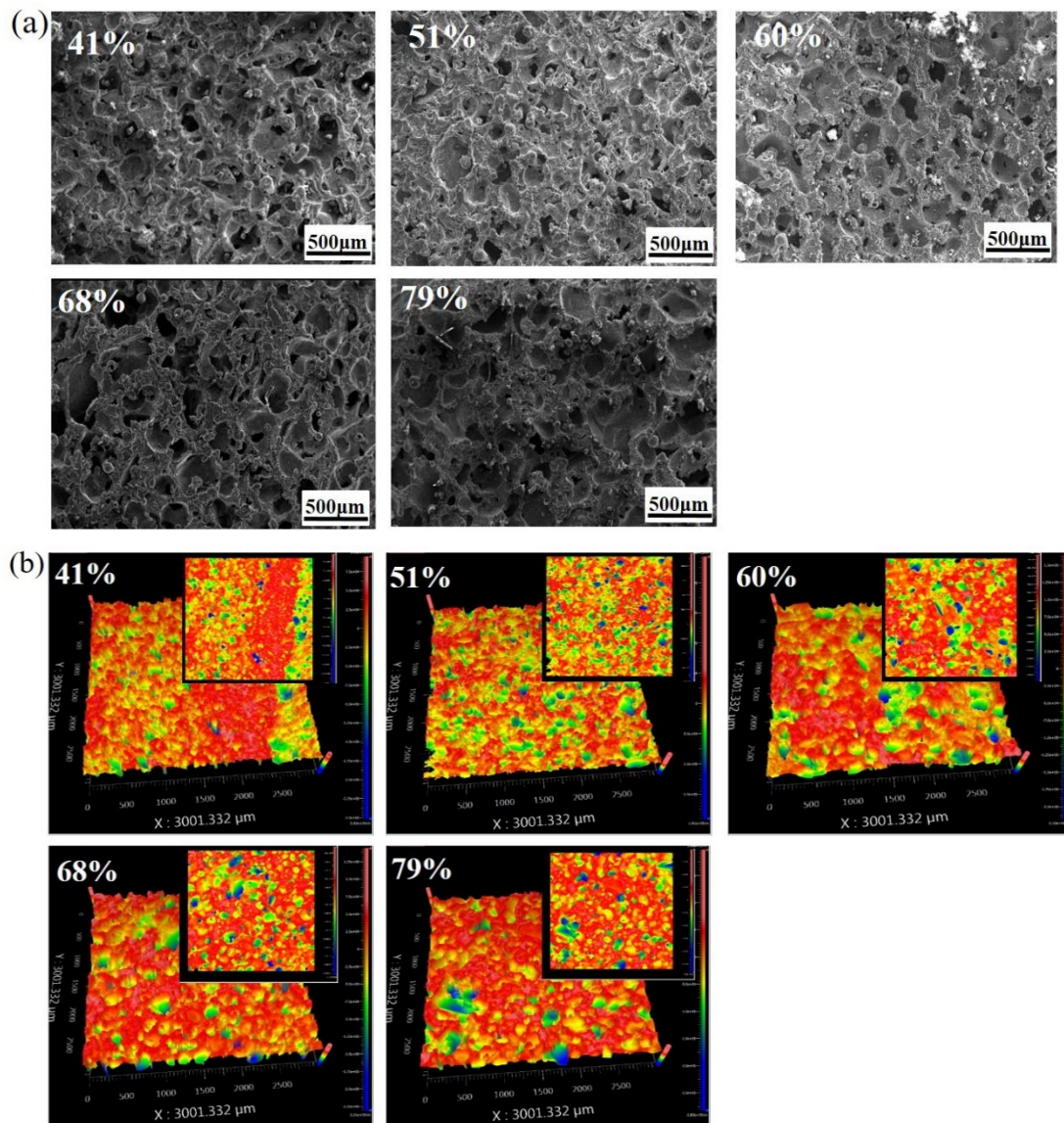


Figure 7. SEM photos (a) and three dimensional photographs of foamed aluminum with different porosity (b)

3.3. Effect of CNTs Mass Fraction on Microstructure of Composites

Figure 8 is a SEM photograph of fractures of composite materials with different mass fractions of CNTs and 60% porosity. It can be seen that the structure and distribution of pores in foamed aluminum and the increase in mass fraction of CNTs have no obvious changes, and can be seen in the fracture morphology. It can be seen that there is a connection between the pores and the pores of the aluminum foam, which belongs to the open-cell small-pore foam aluminum.

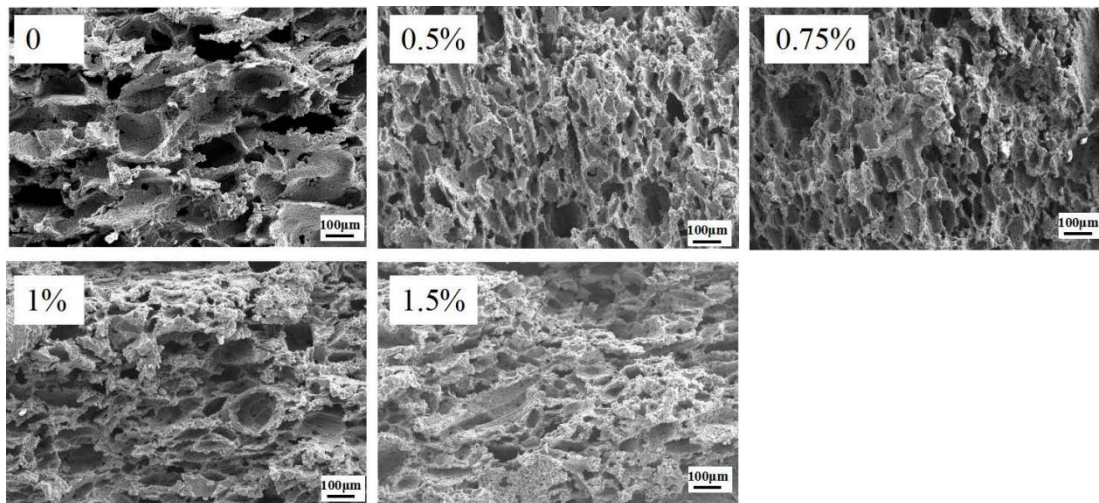


Figure 8. Cross-section SEM photos of aluminum foam with different mass fractions of CNTs

4. Conclusions

(1) CNTs can be effectively dispersed by mixed acid treatment. Compared with the original CNTs, the treated CNTs can maintain one-dimensional nanostructure despite some damage, and new functional groups are introduced into the treated CNTs.

(2) Using NH_4HCO_3 as a pore-forming agent, powder metallurgy can be used to prepare pure aluminum foam with open porosity of 41% ~ 79% and CNTs reinforced aluminum foam composite with 60% porosity.

5. References

- [1] Baumeister J, Banhart J, Weber M. Aluminium foams for transport industry[J]. *Materials & Design*, 1997, 18(4-6): 217-220.
- [2] Jiang J J, Gasik M, Laine J, et al. Electrochemical evaluation of sintered metal hydride electrodes for electric vehicle applications[J]. *Journal of Alloys and Compounds*, 2001, 322(1-2): 0-285.
- [3] Maine E M A, Ashby M F. Applying the investment methodology for materials (IMM) to aluminium foams[J]. *Materials & Design*, 2002, 23(3): 307-319.
- [4] Zhang Yong. Vibrant new functional material foam metal [J]. *Journal of Shandong Institute of engineering*, 1994, 8 (3): 1-6
- [5] Li-hua, TENG, Tian-di, et al. IR study on surface chemical properties of catalytic grown carbon nanotubes and nanofibers[J]. *Journal of Zhejiang University-Science A(Applied Physics & Engineering)*, 2008, 9(5): 720-726.
- [6] Bu Luxia, Wang Chunjie, Yin Lihui, et al. Surface modification and dispersion of multi-walled carbon nanotubes by nitric acid oxidation [J]. *Plating & Finishing*, 2018, 40 (6).
- [7] Qu romeng, Li Yanping, Wang Mei, et al. IR and Raman analysis of acidified MWCNTs [J]. *Chemical engineer*, 2013, 27 (11): 61-63.
- [8] Ma Jianchun, Zhang Jun, Du Peng, et al. Preparation of functionalized modified multi-walled carbon nanotubes [J]. *Shanxi Chemical Industry*, 2015, 35 (2): 12-14.
- [9] Zheng Zheng, Chen Rong, Hu Huating, et al. Research on characterization methods of chemically functionalized modified carbon nanotubes [J]. *Colloid and Polymer*, 2009, 27 (3): 37-40.
- [10] Sood A K, Gupta R, Asher S A. Origin of the unusual dependence of Raman D band on excitation wavelength in graphite-like materials[J]. *Journal of Applied Physics*, 2001, 90(9): 4494.
- [11] Gao Yun, Li Lingyun, Tan Pingheng, et al. Application of Raman spectroscopy in carbon nanotube polymer composites [J]. *Chinese Science Bulletin*, 2010, 55 (22): 2165-2176.